J Neurophysiol 106: 2065–2077, 2011.
First published July 20, 2011; doi:10.1152/jn.01128.2010.

Revisiting the reticulum: feedforward and feedback contributions to motor program parameters in the crab cardiac ganglion microcircuit

Keyla García-Crescioni and Mark W. Miller
Institute of Neurobiology and Department of Anatomy and Neurobiology, University of Puerto Rico Medical Sciences Campus, San Juan, Puerto Rico

Submitted 27 December 2010; accepted in final form 18 July 2011

García-Crescioni K, Miller MW. Revisiting the reticulum: feedforward and feedback contributions to motor program parameters in the crab cardiac ganglion microcircuit. *J Neurophysiol* 106: 2065–2077, 2011. First published July 20, 2011; doi:10.1152/jn.01128.2010.—The neurogenic heartbeat of crustaceans is controlled by the cardiac ganglion (CG), a central pattern generator (CPG) microcircuit composed of nine neurons. In most decapods, five "large" motor neurons (MNs) project from the CG to the myocardium, where their excitatory synaptic signals generate the rhythmic heartbeat. The processes of four "small" premotor neurons (PMNs) are confined to the CG, where they provide excitatory drive to the MNs via impulse-mediated chemical signals and electrotonic coupling. This study explored feedforward and feedback interactions between the PMNs and the MNs in the CG of the blue crab (*Callinectes sapidus*). Three methods were used to compare the activity of the MNs and the PMNs in the integrated CG to their autonomous firing patterns: *1*) ligatures were tightened on the ganglion trunk that connects the PMNs and MNs; *2*) TTX was applied focally to suppress selectively PMN or MN activity; and *3*) sucrose pools were devised to block reversibly PMN or MN impulse conduction. With all treatments, the PMNs and MNs continued to produce autonomous rhythmic bursting following disengagement. Removal of PMN influence resulted in a significantly reduced MN duty cycle that was mainly attributable to a lower autonomous burst frequency. Conversely, after removal of MN feedback, the PMN duty cycle was increased, primarily due to a prolonged burst duration. Application of sucrose to block impulse conduction without eliminating PMN oscillations disclosed significant contributions of spike-mediated PMN-to-MN signals to the initiation and prolongation of the MN burst. Together, these observations support a view of the *Callinectes* CG composed of two classes of spontaneously bursting neurons with distinct endogenous rhythms. Compartmentalized feedforward and feedback signaling endow this microcircuit with syncytial properties such that the intrinsic attributes of the PMNs and MNs both contribute to shaping all parameters of the motor patterns transmitted to the myocardium.

electrical coupling; central pattern generator; driver potential; tetrodotoxin; bursting

CONVERGING EXPERIMENTAL and theoretical advances are producing broadened views of the neuron as the fundamental unit of brain operation (Bullock et al. 2005; Guillery 2007; Kruger and Otis 2007). These reassessments are attributable, in part, to an increased appreciation for the prevalence and consequences of electrical coupling and the complexities of directionality and compartmentalization of neural signaling (Bennett 2002; Bennett and Zukin 2004; Connors and Long 2004; Johnston et al. 2003). Such advances have stimulated increased investigation of information processing at the level of neuronal microcircuits (Grillner and Graybiel 2006; Shepherd and Grillner 2010; Szücs et al. 2009).

Central pattern generator (CPG) networks that control repetitive movements provide advantageous experimental models for examining microcircuit function (Getting 1989; Marder and Calabrese 1996; Wilson et al. 2007). Intensive study of several model CPGs has produced insights into how the intrinsic properties of individual neurons and their synaptic connections generate rhythmic movements (Friesen and Stent 1978; Selverston and Ayers 2006; Selverston 2010). Increasing evidence indicates that electrical coupling as well as compartmentalized and bidirectional signaling also contribute to shaping patterned CPG activity (Evans et al. 2008; Marder 1998; Nusbaum 1994; Perrins and Weiss 1998; Rabbah et al. 2005).

The neurogenic heartbeat of decapod crustaceans is one of the simplest motor systems in which the consequences of reticular network properties can be assessed and quantified. The heartbeat of most crabs and lobsters is controlled by the cardiac ganglion (CG), a CPG microcircuit composed of nine neurons. Four premotor neurons (PMNs) transmit feedforward electrotonic and chemical synaptic signals to five motor neurons (MNs) that project patterned motor drive to the myocardium (Alexandrowicz 1932; Cooke 1988, 2002; Hooper and DiCaprio 2004). Pioneering studies documented the prevalence of electrical coupling and noted the syncytial nature of CG organization (Hagiwara 1961; Maynard 1960; Watanabe and Bullock 1960). Moreover, several observations support a critical contribution of electrotonic MN-to-PMN feedback to the production of rhythmic motor patterns by the CG network (Benson 1980; Berlind 1989; Hartline and Cooke 1969; Sullivan and Miller 1984). This study explored the contributions of feedforward and feedback signaling to shaping parameters of the fictive motor programs produced by the CG of the blue crab (*Callinectes sapidus*). These findings should facilitate molecular and computational approaches to understanding the operation and modulation of this simple CPG-effector motor system (Ball et al. 2010; Hokkanen 2000; Sivan et al. 1999; Stern et al. 2007, 2009; Tobin et al. 2009).

METHODS

Specimens and dissection. All protocols were approved by the Institutional Animal Care and Use Committee of the University of Puerto Rico Medical Sciences Campus (Protocol no. 3220106). Crabs were purchased from local fishermen at the San José Lagoon in Isla Verde, Puerto Rico. Hearts were pinned ventral side up in Sylgard-lined petri dishes. A cut was made in the ventral musculature exposing the CG. Dissection was achieved principally by teasing away the

Address for reprint requests and other correspondence: M. W. Miller, Institute of Neurobiology, Univ. of Puerto Rico, 201 Blvd. del Valle, San Juan, PR 00901 (e-mail: mark.miller@upr.edu).

adhering myocardium. Small, noncontracting remnants of muscle were retained to preserve the dendritic endings of CG neurons that project into the confluence between the motor roots at the anterior and posterior ends of the ganglion (Fort et al. 2004; García-Crescioni et al. 2010; Tazaki and Cooke 1979a).

Electrophysiology. Membrane potentials were recorded from anterior and/or posterior MNs using 2 M KCl-filled microelectrodes (10–30 MΩ; Fig. 1*A*). Higher-resistance (>20-MΩ) electrodes were used to record from PMN somata. In portunid crab species, electrical coupling among the neurons of the CG produces precisely synchronized activity in each of the five MNs (Fig. 1*A*; see Berlind 1982; Fort et al. 2004; Tazaki 1972; Tazaki and Cooke 1979a). The generation of CG bursts is promoted by intrinsic, prolonged, local TTX-resistant depolarizing potentials, termed driver potentials (DPs; Tazaki and Cooke 1979b,c, 1983a–c). When recordings from anterior and posterior MNs are compared, all electrical signals (synaptic potentials, slow potentials, and action potentials) are larger in the anterior MNs (Fig. 1*A*), indicating that these signals originate in the anterior portion of the ganglion and are more attenuated at the posterior end.

Extracellular recordings were acquired with a Teflon-coated silver wire inserted into a small Sylgard platform supporting the ganglion (Fig. 1*A*). The trunk of the ganglion was positioned over a small depression in the Sylgard platform that contained the exposed wire tip. Pools fashioned from petroleum jelly (Vaseline) around various portions of the CG (see Figs. 1 and 3–9) provided sufficient electrical resistance to enable differential recording of total ganglion trunk activity. In such trunk recordings, the PMN impulse amplitudes were typically <15% of those generated by the MNs. PMN firing initiated each burst and continued after the termination of MN firing (Fig. 1*A*, compare dashed vertical lines and dotted vertical lines).

The Vaseline pools also made it possible to change the composition of the bathing solution surrounding specific regions of the ganglion. The crab saline composition was based on Pantin saline for *Cancer pagurus*: 487 mM NaCl, 13.6 mM KCl, 13.4 mM $CaCl_2$, 13.6 mM $MgCl_2$, 1.4 mM sodium sulfate, 3 mM HEPES, adjusted to pH 7.4 with sodium hydroxide (see Krajniak 1991). Preparations were continuously superfused with saline (2 ml/min, 20–22°C). Solution changes inside the well were performed manually with a 10-μl pipette. TTX (Sigma-Aldrich) was prepared in crab saline, and sucrose (Sigma-Aldrich) was dissolved in distilled water (see Abbott et al. 1975; Russell 1979).

Data analysis. All results reported in this study were observed in ≥4 specimens. Measurements are reported as means ± SD. For ligature experiments, statistical tests (Student's *t*-test, 2-tailed) were performed by comparing measurements obtained before the procedure to those observed 20–30 min following ligature. For experiments with TTX and sucrose, a 1-way ANOVA was initially applied to test overall significance, and Holm-Sidak post hoc tests were used to

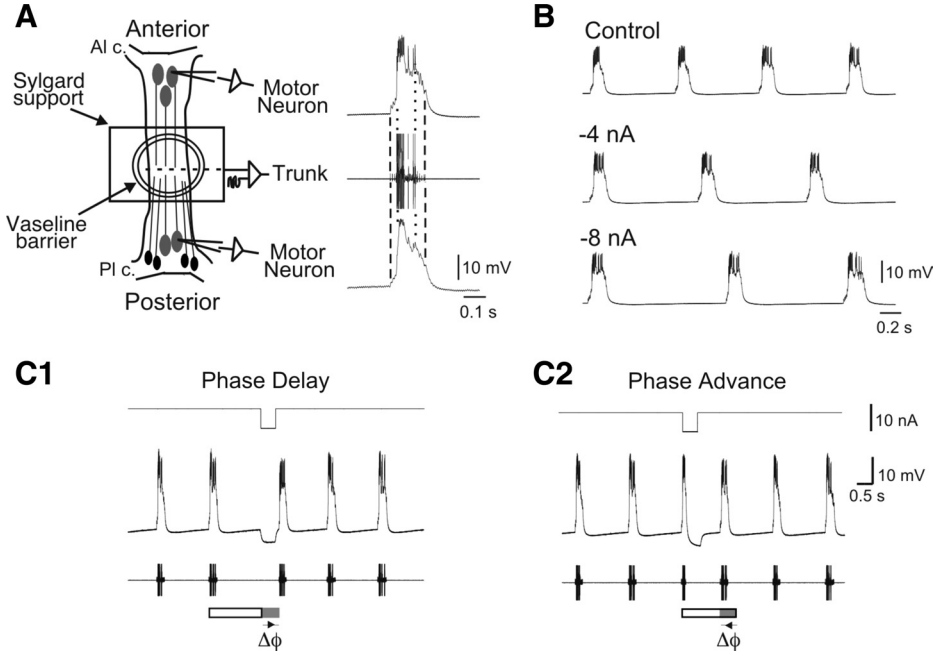

Fig. 1. Electrophysiological protocols and properties of the *Callinectes* cardiac ganglion (CG). *A*, *left*: schematic diagram of the CG showing the methods used in this study. The ganglion contains 5 motor neurons (MNs; 3 anterior and 2 posterior, shaded gray) and 4 smaller posterior premotor neurons (PMNs; shaded black). The axons of all MNs are oriented toward the trunk so that the posterior MNs project out the anterolateral connectives (Al c.) and the anterior MNs project to the posterolateral connectives (Pl c.; see García-Crescioni et al. 2010). The axons of the 4 PMNs project toward the anterior end but remain within the CG trunk. The CG was pinned spanning a small (approximately 2 × 2 × 3 mm) Sylgard support in which a molded depression contained the exposed end of a Teflon-coated recording electrode (dashed line). A Vaseline barrier was fashioned around the depression to isolate the electrode and to enable selective application of TTX or sucrose to a limited portion of the CG trunk (midregion shown here). *A*, *right*: differential alternating current (AC) recording captures signals from all CG neurons as they pass through the central trunk. MN signals were typically 10–15× greater than the PMNs. As all 5 MNs fire in precise synchrony (see Fort et al. 2004), the MN spikes recorded from the trunk correspond 1 for 1 with the impulses recorded from any of the 5 MNs (cf. anterior MN). Within each burst, PMN activity (delimited by vertical dashed lines) both preceded and followed MN firing (dotted lines). In simultaneous intracellular direct current (DC) recordings acquired with glass microelectrodes from the inexcitable MN cell bodies, all signals [PMN-to-MN excitatory postsynaptic potentials (EPSPs), MN impulses, and slow burst-forming potentials] are larger in the anterior MNs compared with posterior MNs, indicating that they originate in the anterior portion of the ganglion. *B*: intracellular recording from an anterior MN exhibits rhythmic burst activity under control conditions. Injection of continuous hyperpolarizing current (−4 and −8 nA) via a 2nd microelectrode into the soma of a posterior MN reduced the frequency of CG bursting. *C*: recording from anterior MN. Injection of hyperpolarizing current pulses (8 nA, 0.5 s) into a posterior MN produced a phase delay (C_1) or phase advance (C_2) of the subsequent burst, depending on the timing of the pulse. The predicted periods, based on the previous 5 cycles, are indicated by bars below the recordings (white fill, dark outline). Gray bars indicate the delay and advance of the subsequent burst.

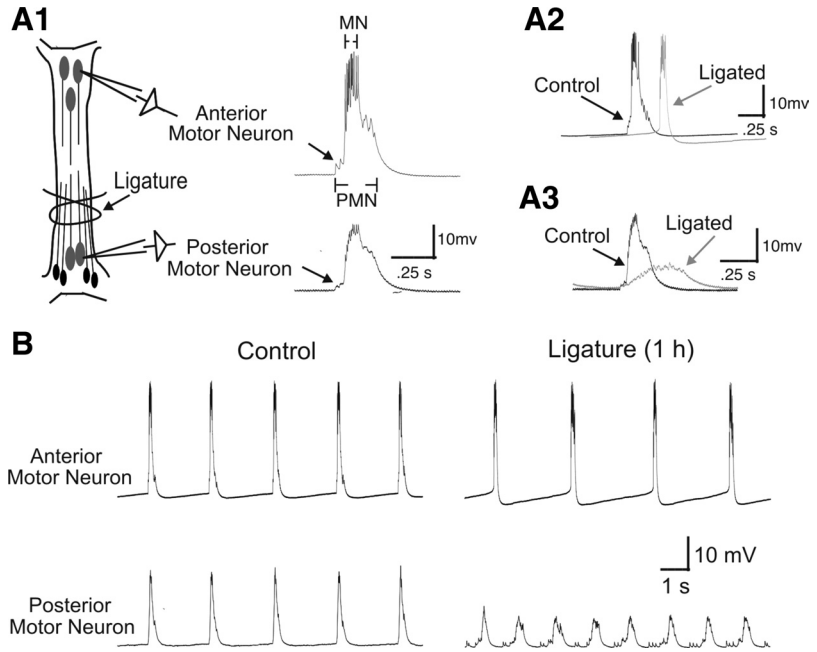

Fig. 2. Dissociation of MN and PMN electrical activity following ligature of the CG trunk. A_1, *left*: schematic drawing of the CG and the protocol used to assess effects of trunk ligature. A ligature (hair from a golden retriever) is shown tied loosely around the trunk, as configured during control recordings. The microelectrodes were withdrawn from the anterior and posterior MNs before tightening the ligature. They were then reintroduced to the same cells, and the preparation was allowed 1 h to stabilize. A_1, *right*: under control conditions, all synaptic (arrows) and impulse activity in the anterior MN (*top* recording) was recorded in a more attenuated form in the posterior MN (*bottom* recording). The MN burst (indicated above anterior recording) was preceded and followed by EPSP activity reflecting the PMN burst (indicated below anterior MN recording). A_2: following ligature, anterior MNs continued to burst (compare gray ligated record superimposed on black control burst). However, no EPSPs were detected in recordings from anterior somata, and their burst durations were reduced. A_3: although the posterior MN ceased to burst following ligature, small (3–10 mV) depolarizing potentials (gray recording), reflecting electrically coupled PMN burst activity, were recorded from the posterior MN somata (see Miller et al. 1984; Tazaki and Cooke 1983a). *B*: simultaneous recordings demonstrate synchronous rhythmic bursting in an anterior MN and a posterior MN before ligature (control). Following ligature, bursting in the anterior MN was highly rhythmic but slower than under control conditions. The PMN bursts, monitored via recording from a posterior MN, were uncoupled from the anterior MNs. In contrast to the anterior MNs, the PMN burst rate was greater than the control rhythm.

compare control, experimental, and washout conditions. A value of $P < 0.05$ was established as the criterion for significance.

RESULTS

Current injection into MNs. Two sets of observations showed that manipulation of the MN membrane potential could influence the rhythmic activity of the *Callinectes* CG, as observed previously in other decapods (Benson 1980; Mayeri 1973a,b; Tazaki 1972; Tazaki and Cooke 1979a, 1983a). First, injection of continuous hyperpolarizing current into a posterior MN via an intrasomatic microelectrode reduced the CG burst frequency, as monitored via a second microelectrode recording from an anterior MN (Fig. 1*B*). Second, pulses (8 nA, 500 ms) of hyperpolarizing current injected into a posterior MN produced phase delays (Fig. 1C_1) or phase advances (Fig. 1C_2) of the subsequent burst depending on the timing of the stimulus (see Benson 1980). These observations indicate that feedback from the MNs to the PMNs contributes to shaping the motor patterns of the *Callinectes* CG. The following experimental manipulations were therefore devised to compare the activity of the CG MNs and PMNs in the integrated CG to their behavior following elimination of their reciprocal influence.

Ligature of the CG trunk. Tazaki and Cooke (1983a) used ligatures to explore the topographic localization of burst-forming and rhythm-generating loci in the CG of the portunid crab (*Portunus sanguinolentus*). When ligatures were placed near the midpoint of the ganglion, disengaging the anterior MNs from the posterior PMNs, they observed that the three anterior MNs exhibited spontaneous rhythmic burst activity. We initially conducted similar ligature experiments *1*) to determine whether the CG of *Callinectes* exhibits a topographic organization similar to that of *Portunus*, and *2*) to quantify the parameters of MN burst activity when dissociated from the influence of the PMNs.

Ligatures placed slightly posterior to the midpoint of the *Callinectes* CG reliably removed the influence of the PMNs on the three anterior MNs (Fig. 2, A_2 and *B*). The excitatory postsynaptic potentials (EPSPs) that preceded and followed anterior MN bursting under control conditions were eliminated, and several parameters of the anterior MN burst were modified following trunk ligature. The MN burst duration, measured as the time between its initial and final impulses (Fig. 2A_1), was significantly reduced (control: 135.3 ± 46.2 ms, ligated: 30.2 ± 11.6 ms; $n = 6$; $P < 0.05$; Figs. 2A_2 and 3A_1), as was the number of impulses per burst (control: 5.3 ± 2.1, ligated: 3.1 ± 1.5; $n = 7$; $P < 0.05$; Figs. 2A_2 and 3A_2).

The membrane potential during the interburst interval (IBI) exhibited a steeper average slope following the ligation (control: 0.50 mV/s; ligated: 1.16 mV/s; $n = 5$ preparations). Despite this enhanced trajectory, the IBI of the dissociated anterior MNs was significantly increased (control: 1.44 ± 0.24 s, ligated: 2.83 ± 0.93 s; $n = 6$; $P < 0.05$; Fig. 2*B*, *top* recordings). The increased IBI and decreased burst rate observed in the anterior MNs following ligation [control: 35.2 ±

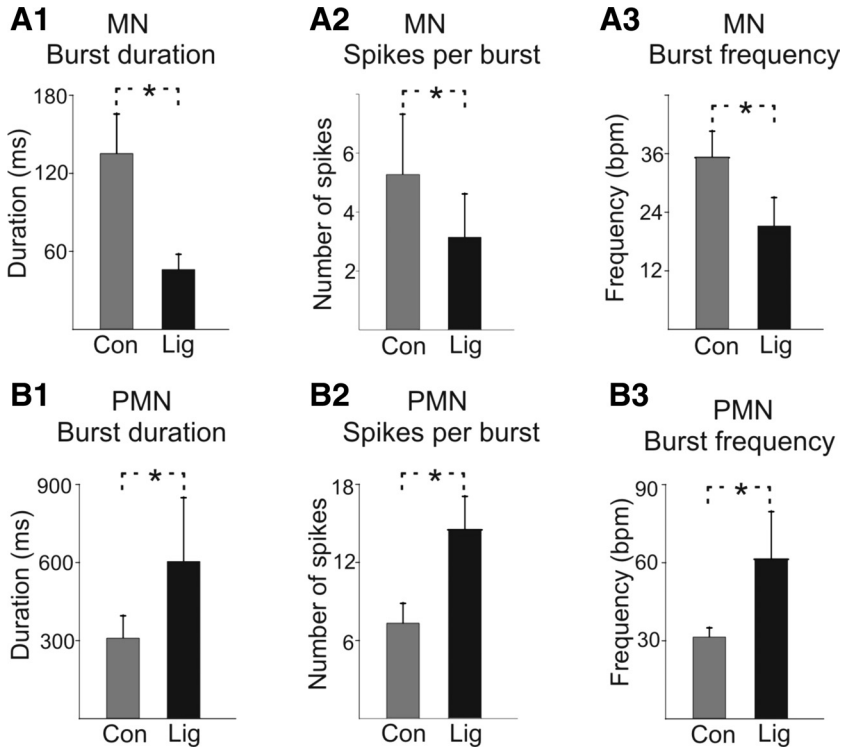

Fig. 3. Group data summarizing effects of trunk ligature on MN and PMN activity. Data were collected 1 h following tightening of ligature around the CG trunk ~200 μm anterior to the posterior MN cell bodies (Fig. 2, A_2 and B, *top* records). A_1: the MN burst duration was decreased following ligature ($t = 5.413$, $P < 0.05$). A_2: the number of impulses comprising the MN bursts was reduced following ligature ($t = 2.234$, $P < 0.05$). A_3: burst activity recorded from anterior MNs occurred at a lower frequency after ligature ($t = 4.747$, $P < 0.05$). B: PMN activity was recorded via its electrical coupling to the PMNs, which were silenced by the ligature (Fig. 2, A_3 and B, *bottom* traces). B_1: the PMN burst duration increased after ligature ($t = 4.358$, $P < 0.05$). B_2: the number of impulses comprising each PMN burst was increased following ligature ($t = 8.248$, $P < 0.05$). B_3: PMN burst activity occurred at a higher frequency after ligature ($t = 3.948$, $P < 0.05$). *$P <$ 0.05, Student's *t*-test, 2-tailed. Con, control; Lig, ligature; bpm, bursts per minute.

5.4 bursts per minute (bpm), ligated: 21.9 ± 5.8 bpm; $n = 8$; $P < 0.05$; Figs. 2*B* and 3A_3] could be attributed, at least in part, to an augmented postburst hyperpolarization that caused the ligated anterior MNs to attain more negative membrane potentials (Fig. 2, A_2 and B; control = −47.2 mV; ligated: −50.4 mV; $n = 5$; $P < 0.05$). No differences in the threshold for burst initiation were detected (Fig. 2A_2).

Trunk ligature achieved a complete elimination of electrical coupling between the anterior and posterior MNs. As shown previously in *Portunus* (Miller et al. 1984; Tazaki and Cooke 1983a), such dissociation of the posterior MNs reveals the activity of the PMNs, as their electrical coupling occurs predominantly within the posterior half of the CG trunk (Fig. 2, A_3 and B, *bottom* recordings). The amplitude of the coupled PMN activity recorded from a posterior MN soma following ligature ranged from 3 to 10 mV with small (0.5–1 mV), rapid superimposed inflections corresponding to the PMN impulses. When these potentials were compared with control preligature PMN bursts, they were found to exhibit longer durations (control: 310.0 ± 85.3 ms, ligated: 604.1 ± 245.2 ms; $n = 7$; $P < 0.05$; Fig. 2, A_3 and B, and Fig. 3B_1), more PMN impulses per burst (control: 7.3 ± 1.5, ligated: 14.5 ± 2.6; $n = 7$; $P < 0.05$; Fig. 3B_2), and increased rates (control: 31.5 ± 3.5 bpm, ligated: 61.3 ± 18.3 bpm; $n = 7$; $P < 0.05$; Fig. 2*B*, *bottom* recordings, and Fig. 3B_3).

Silencing PMNs and MNs with TTX. The efficacy of ligature experiments reflects the physical interruption of axonal impulse conduction in all neurons that traverse the CG trunk. Such acute treatments could produce additional effects due to the responses of ligatured MNs neurons to injury (see Saver et al. 1999) or damage to regulatory fibers that originate from the CNS and innervate the CG (Delgado et al. 2001; Fort et al. 2004). Moreover, as it is not possible to reverse the effects of ligatures, we sought alternative manipulations that could achieve our objective of dissociating PMN and MN activity.

TTX has been shown to block impulses in the cardiac ganglia of crabs and lobsters (Sullivan and Miller 1984; Tazaki 1971; Tazaki and Cooke 1979b). To assess the effects of silencing the PMNs, a Vaseline barrier was constructed around the posterior region of the ganglion (Fig. 4A_1). When the solution within the pool was removed and replaced with saline containing 1 μM TTX, the synaptic influence of the PMNs on the three anterior MNs was eliminated (Fig. 4, A_1 and A_2). Although burst activity persisted in the MNs, there was a significant reduction in its duration (control: 165.6 ± 83.2 ms, TTX: 45.2 ± 21.3 ms; $n = 6$; $P < 0.05$). This effect was incompletely reversed following 1-h wash with TTX-free solution (wash: 118.0 ± 102.6 ms; Fig. 4, A_1 and B_1; $P > 0.05$). The reduced burst duration was accompanied by an increase in the amplitude of the slow potential underlying the MN burst (measured from the resting V_m to the most hyperpolarized potential of the superimposed impulses; control: 8.0 ± 3.1 mV, TTX: 14.2 ± 4.0 mV; $n = 6$; $P < 0.05$). No change in the number of MN impulses per burst was detected (control: 7.3 ± 2.4, TTX: 7.2 ± 3.4, wash 5.0 ± 2.8; $n = 6$; $P > 0.05$).

As observed following trunk ligature, the rate of MN bursting was significantly reduced after silencing the PMNs with TTX (control: 32.7 ± 7.9 bpm, TTX: 18.8 ± 6.3 bpm, wash: 36.0 ± 13.2 bpm; $n = 6$; $P < 0.05$; Fig. 4, A_2 and B_2). Moreover, the average trajectory of depolarization during the IBI was again increased (control: 0.4 mV/s; TTX: 0.8 mV/s; $n = 6$ preparations). In contrast to the ligature treatment, the MN membrane potential was depolarized by an average of 4.5 ± 0.8 mV following posterior TTX application ($n = 6$). The reduced MN burst duration and increased period contributed to a significant reduction in the MN duty cycle (control:

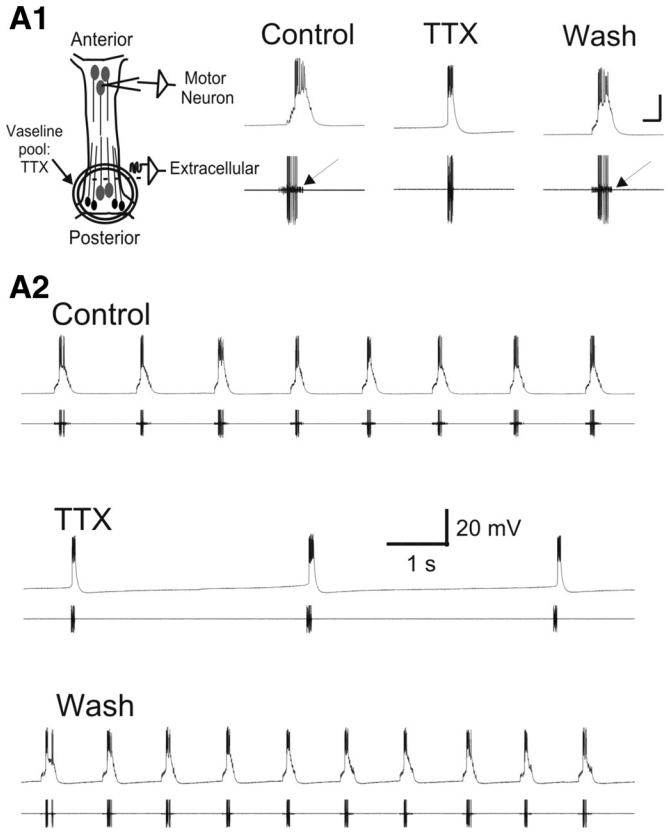

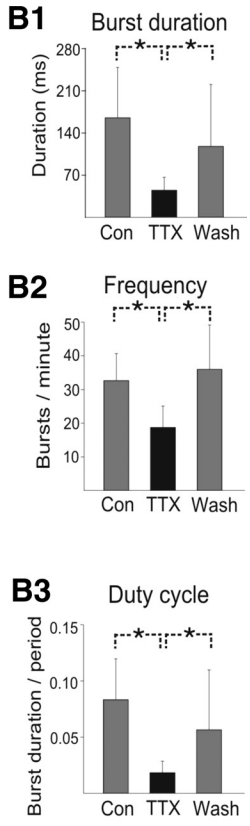

Fig. 4. Effect of silencing of posterior neural activity with TTX. A_1: TTX (1×10^{-6} M) was introduced to a Vaseline pool constructed around the posterior end of the CG. Ganglion activity was recorded intracellularly from an anterior MN and extracellularly from the ganglion trunk between electrodes placed within and outside of the pool. Small PMN impulses observed in the extracellular recording (Control, arrow) were eliminated in the presence of TTX. Although EPSPs were no longer present in the anterior MN, it continued to produce bursts. Following 1-h wash with normal solution, the PMN impulses were partially restored (Wash, arrow). A_2: bursting by an anterior MN after silencing the posterior neurons with TTX was less frequent than control conditions. B_1: summary data from 6 experiments show that the duration of anterior MN bursts was significantly and reversibly reduced following silencing the posterior neurons with TTX (ANOVA; $F_{2,15} = 3.693$). B_2: group data show that the frequency of anterior MN bursting was significantly and reversibly reduced following silencing the posterior neurons with TTX (ANOVA; $F_{2,15} = 5.440$). B_3: the reduced burst duration (B_1) and burst frequency (B_2) contributed to a significant reduction in the duty cycle of anterior MN bursting (ANOVA; $F_{2,18} = 5.308$). $^*P < 0.05$, Holm-Sidak pairwise post hoc tests.

0.08 ± 0.04, TTX: 0.02 ± 0.01, wash: 0.06 ± 0.05; $n = 7$; $P < 0.05$; Fig. 4, A_2 and B_3).

Vaseline partitions surrounding the anterior portion of the ganglion were used to silence selectively the MNs with TTX (Fig. 5A_1). Within 8–10 min of replacing the solution within the barrier with saline containing TTX (1×10^{-6} M), the MN impulses were completely eliminated. Bursts of PMN impulses recorded extracellularly across the resistance of the Vaseline corresponded to the depolarizing potentials recorded intracellularly from a posterior MN (Fig. 5A_1, *middle* records, TTX). As it was not possible to discriminate individual units originating from the four PMNs, burst parameters were measured from their collective activity. Elimination of MN activity resulted in a significant increase in the duration of the PMN burst (control: 272.9 ± 85.7 ms, TTX: 444.8 ± 129.4 ms; $n = 7$; $P < 0.05$; Fig. 5, A_1 and B_1) that was partially reversed following 1-h wash (303.7 ± 107.3 ms; $P > 0.05$). The number of impulses per PMN burst was concomitantly increased (control: 13.3 ± 6.9; TTX: 26.5 ± 7.1; wash: 15.1 ± 7.4; $n = 8$; $P < 0.05$; Fig. 5, A_1 and B_2).

After silencing MNs with TTX, PMN bursting exhibited some trend to become more rapid (control: 33.1 ± 10.2 bpm, TTX: 42.0 ± 11.1 bpm), but this tendency was not completely reversed with 1-h wash (36.4 ± 10.9 bpm) and did not reach our criterion for statistical significance ($F_{2,30} = 1.939$; $P = 0.16$; Fig. 5A_2). The significant increase in the PMN duty cycle produced by silencing the MNs with TTX (control: 0.18 ± 0.05, TTX: 0.37 ± 0.10, wash: 0.24 ± 0.09; $n = 8$; $P < 0.05$; Fig. 5, A_2 and B_3) was therefore attributed primarily to the increased burst duration.

Blockade of impulse conduction with sucrose. As prolonged periods of wash (>1 h) were insufficient to reverse some effects observed with TTX, alternative methods were sought to suppress PMN and MN impulse activity. Replacement of the saline within the Vaseline partition with a 750 mM sucrose solution was found to produce a blockade of impulse conduction that was completely reversed within 10–15 min following return to normal saline. Addition of sucrose to a pool surrounding the posterior end of the CG selectively eliminated PMN firing within 1 min (Fig. 6A_1). As observed following silencing the PMNs with TTX, spontaneous burst activity persisted in the MNs (Fig. 6, A_1 and A_2). On elimination of synaptic drive, there was a significant reduction in the MN burst duration (control: 94.2 ± 26.4 ms, sucrose: 47.6 ± 25.6 ms; $n = 5$; $P < 0.05$). This effect of sucrose was completely reversed with normal crab Ringer (wash: 108.6 ± 30.1 ms; $P < 0.05$; Fig. 6, A_1 and B_1). As with TTX, the reduced duration of the spontaneous MN burst was not associated with a decrease in the number of impulses per burst (control: 6.4 ± 0.9, sucrose: 6.3 ± 2.4, wash 7.0 ± 1.9; $n = 6$; $P > 0.05$).

Repetitive bursting of the anterior MNs was highly rhythmic after application of sucrose to the posterior neurons (Fig. 6A_2). Although the average rate of depolarization during the IBI was increased (control: 0.50 mV/s; sucrose: 0.88 mV/s; $n = 5$ preparations), the rate of MN bursting was significantly reduced (control: 35.9 ± 7.8 bpm, sucrose: 13.6 ± 6.0 bpm, wash: 31.1 ± 8.4 bpm; $n = 5$; $P < 0.05$; Fig. 6B_2). The reduced MN burst duration and increased period contributed to a significant reduction in the MN duty cycle (control: 0.06 ± 0.04, sucrose: 0.01 ± 0.00, wash: 0.06 ± 0.02; $n = 7$; $P < 0.05$; Fig. 6B_3).

Application of sucrose to the anterior portion of the ganglion eliminated MN activity (Fig. 7A_1). Within 2–3 min of replacing the solution within the barrier with saline containing sucrose

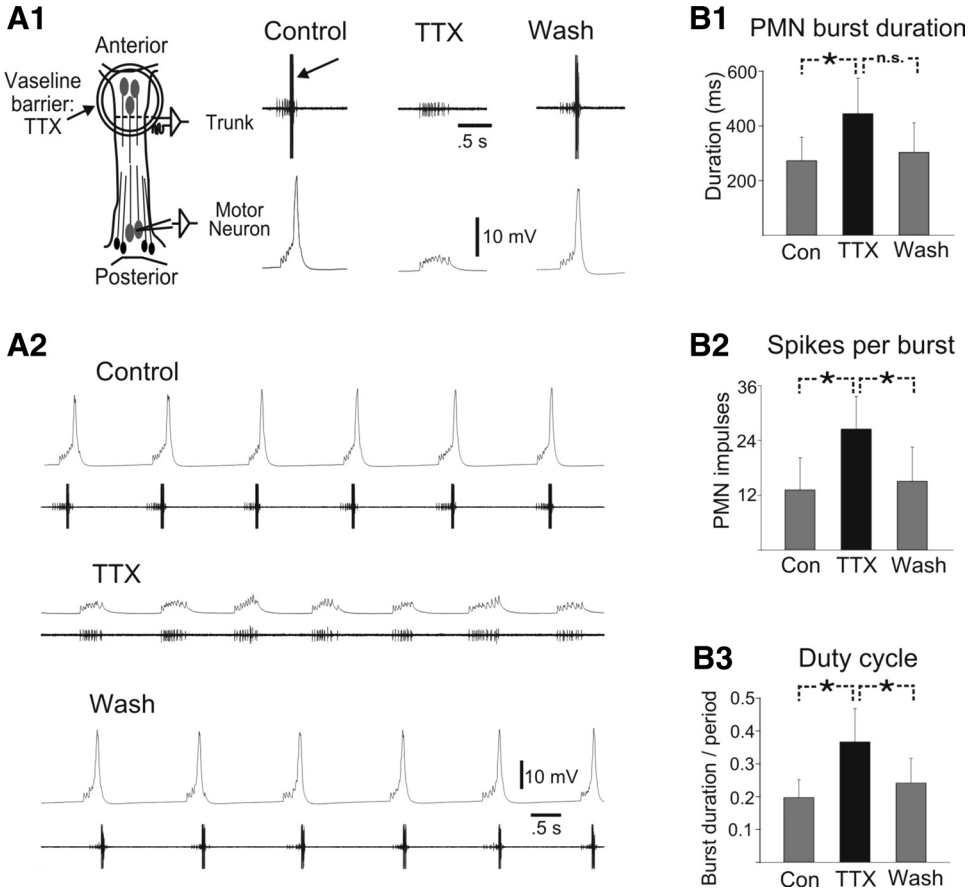

Fig. 5. Effect of silencing MN activity with TTX. A_1 and A_2: TTX (1×10^{-6} M) was introduced within a Vaseline barrier constructed around the anterior end of the CG. Ganglion activity was recorded intracellularly from a posterior MN and extracellularly from the ganglion trunk between wire electrodes placed within and outside of the pool. Large MN impulses observed in the extracellular recording (Control, arrow) were eliminated in the presence of TTX. Although the posterior MN ceased firing, it continued to exhibit rhythmic depolarizing potentials corresponding to PMN bursts recorded from the trunk. Following 1-h wash with normal saline, the MN impulses were partially restored (Wash). B_1: summary data from 7 experiments show that the duration of PMN bursts was significantly increased following silencing the MNs with TTX (ANOVA; $F_{2,18} = 4.960$). Following 1-h wash, the effect of TTX on the PMN burst duration was not completely reversed ($P > 0.05$). B_2: group data from 8 experiments show that the number of PMN impulses per burst is significantly and reversibly increased following silencing the MNs with TTX (ANOVA; $F_{2,21} = 8.000$). B_3: the increased duration (B_1) and burst frequency contribute to producing a significant increase in the duty cycle of PMN bursting (ANOVA; $F_{2,21} = 8.970$). *$P < 0.05$, Holm-Sidak pairwise post hoc tests. n.s., Not significant.

(750 mM), the MN impulses were completely abolished. The PMN impulses recorded extracellularly were substantially larger than those observed under control conditions, probably due to the increased resistance of the medium (Fig. 7, A_1 and A_2, *middle* records). As with TTX, however, it was not possible to discriminate units originating from the four individual PMNs. Elimination of MN activity resulted in a significant increase in the duration of the collective PMN burst (control: 245 ± 70 ms, sucrose: 415 ± 84 ms, wash: 224 ± 88 ms; $n = 9$; $P < 0.05$; Fig. 7, A_1 and B_1) and an increase in the number of impulses per PMN burst (control: 11.5 ± 6.4; sucrose: 27.0 ± 9.7; wash: 13.0 ± 6.3; $n = 10$; $P < 0.05$; Fig. 7, A_1 and B_2).

After silencing the MNs with sucrose, the frequency of PMN bursting did not change sufficiently (control: 32.0 ± 10.8 bpm, sucrose: 40.0 ± 14.3 bpm, wash: 35.7 ± 14.6 bpm) to reach our criterion for statistical significance ($F_{2,18} = 0.630$, $P = 0.54$; Fig. 7A_2). The significant increase in the PMN duty cycle (control: 0.20 ± 0.04, sucrose: 0.30 ± 0.08, wash: 0.20 ± 0.05; $n = 10$; $P < 0.05$; Fig. 7, A_2 and B_3) was thus attributed primarily to the increase in burst duration.

Intracellular recording was achieved from PMNs in two experiments in which MNs were silenced with sucrose (Fig. 8). Under control conditions, the duration of the *Callinectes* PMN bursts was greater than MN bursts, and the IBI exhibited a more prominent pacemaker potential (Fig. 8, A_1 and A_2), as observed in the cardiac ganglia of other decapods (Tameyasu 1976; Tazaki and Cooke 1979a). PMN firing reached its highest frequency during the MN burst and ceased shortly after termination the MN burst (Fig. 8, *A* and *B*). When MN firing was blocked by addition of sucrose to the anterior portion of the ganglion, the most apparent effect was an increased duration of the PMN burst (Fig. 8*B*). However, the maximal intraburst firing frequency was reduced. These findings are in agreement with observations on the collective PMN activity following silencing MNs with either TTX (Fig. 5) or sucrose (Fig. 7). Together, they indicate that the MN burst exerts both excitatory and inhibitory influences that contribute to shaping PMN firing patterns (see DISCUSSION).

Finally, the efficacy and reversibility of the actions of sucrose enabled us to assess the relative contributions of anterior vs. posterior feedforward PMN-to-MN signaling to the control of CG motor activity. Addition of sucrose to a chamber surrounding the middle part (approximately ⅓) of the CG (Fig. 9*A*) did not block PMN bursting, but it did prevent impulse conduction to the anterior synaptic region. Under these conditions, depolarizations produced by PMN bursts in anterior MNs were more attenuated than those recorded in the posterior MNs (Fig. 9*A*; cf. Figs. 1A_1 and 2A_1). This reflects features of CG functional topography shown with ligatures in other portunid crabs (Tazaki and Cooke 1983a) and in Fig. 2 of this report: *1*) chemical PMN-to-MN synaptic signaling, which occurs in the anterior half of the trunk, is eliminated with application of sucrose to the trunk; *2*) electrical coupling between the PMNs and posterior MNs, which occurs predominantly in the posterior region of the ganglion, persists with sucrose application to the trunk; and *3*) PMN-to-MN electrical coupling passes slowly changing signals, e.g., DPs, more effectively than rapid ones, e.g., impulses (see Figs. 2, 5, and 7 of this paper).

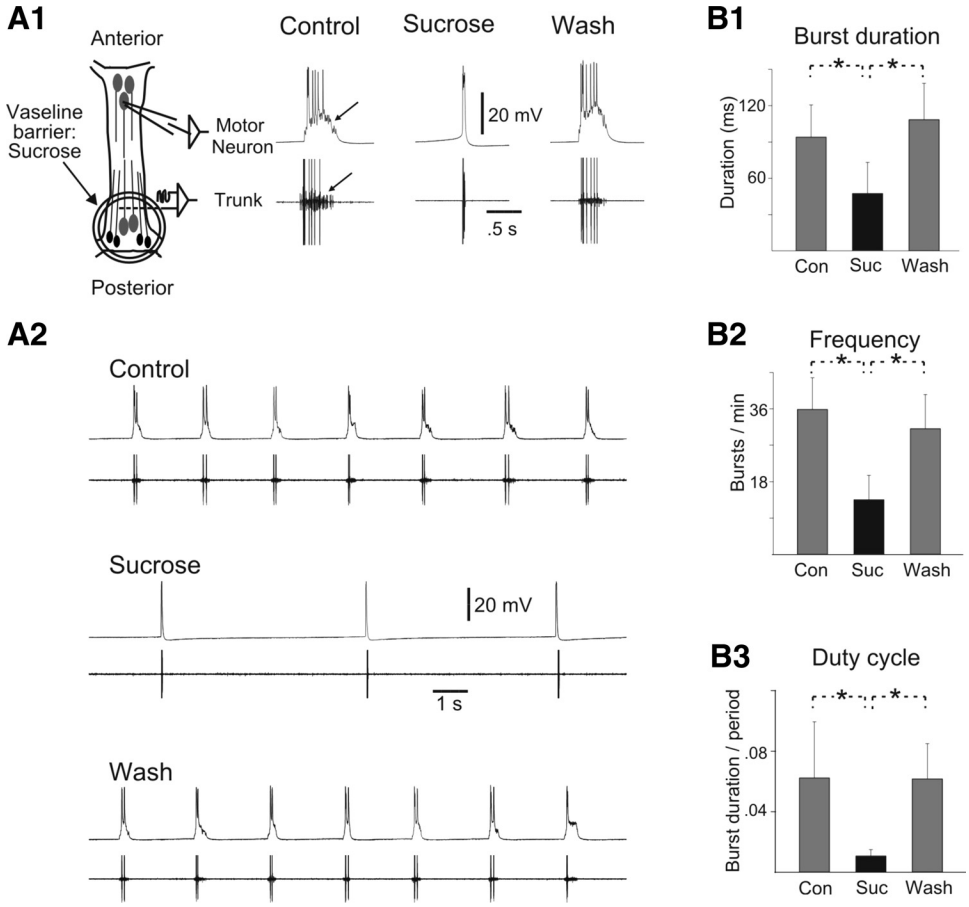

Fig. 6. Effects of silencing posterior neurons with sucrose. A_1: sucrose (750 mM) was introduced within a Vaseline barrier constructed around the posterior end of the CG. Ganglion activity was recorded intracellularly from an anterior MN and extracellularly from the ganglion trunk between electrodes placed within and outside of the partition. Small PMN impulses observed in the extracellular recording correspond to EPSPs in the intracellular recording (Control, arrows). Both were eliminated in the presence of sucrose. Although the MN no longer received synaptic drive, it continued to produce bursts of brief duration. Following 10- to 15-min wash with normal solution, the PMN impulses were restored (Wash). A_2: repetitive bursting by an anterior MN after silencing the posterior neurons with sucrose was less frequent than in control conditions. B_1: summary data from 5 experiments show that the duration of anterior MN bursts was significantly and reversibly reduced following silencing the posterior neurons with sucrose (ANOVA; $F_{2,12} = 6.757$). B_2: group data from 5 experiments show that the frequency of anterior MN bursting was significantly and reversibly reduced following silencing the posterior neurons with sucrose (ANOVA; $F_{2,12} = 12.363$). B_3: the reduced burst duration (B_1) and burst frequency (B_2) contributed to a significant reduction in the duty cycle of anterior MN bursting (ANOVA; $F_{2,18} = 9.574$). $^*P < 0.05$, Holm-Sidak pairwise post hoc tests.

Although some PMN bursts caused the MNs to reach threshold for bursting, others did not. Ganglia typically exhibited a regular pattern in which every third or second PMN burst caused MN bursting (Fig. 9*A*). The intermittent ability for PMN firing to cause MN bursts resulted in decreased MN burst rates (control period: 1.87 ± 0.48 s, sucrose: 2.78 ± 0.86 s; $n = 6$; $P < 0.05$; Fig. 9B_1). When MN bursts did occur, they were briefer than those observed before suppressing PMN impulse conduction (control: 100.3 ± 41.1 ms, sucrose: 51.9 ± 20.3 ms; $n = 7$; $P < 0.05$; Fig. 9B_1). Thus, although these observations demonstrate the ability of slow electrotonic signals to drive MN bursts, they also underscore the crucial contribution of impulse-mediated chemical synaptic signaling to sustaining the rate and duration of MN bursts.

Following block of impulse conduction through the trunk with sucrose, PMN burst rates were increased, with IBI being reduced to the same extent whether MN bursts were elicited or not (control: 1.61 ± 0.26 s, sucrose with MN burst: 1.16 ± 0.13 s, sucrose without MN burst: 1.05 ± 0.15 s; $n = 5$; $P < 0.05$; Fig. 9B_2). The duration of the PMN bursts, on the other hand, were only prolonged in those instances when MN bursts did not occur (control: 293.2 ± 38.4 ms, sucrose with MN burst: 281.4 ± 75.5 ms, sucrose without MN burst: 399.2 ± 78.3 ms; $n = 5$; $P < 0.05$; Fig. 9B_2). This finding agrees with our observations following silencing the MNs with TTX (Fig. 5) and sucrose (Fig. 7) and supports the hypothesis that electrotonic MN-to-PMN feedback participates in the termination of PMN bursts (see DISCUSSION).

DISCUSSION

These experiments were designed *1*) to determine the intrinsic activities of the PMNs and MNs in the *Callinectes* CG, and *2*) to explore the contributions of feedforward and feedback signaling to the generation of motor patterns by the integrated network. Three independent methods, trunk ligature, TTX, and sucrose, were implemented to eliminate signaling between the PMNs and MNs, permitting comparisons between their autonomous activity and their behavior in the integrated network (Tables 1 and 2). Although the results of the three protocols were generally complementary, trunk ligatures produced two effects, decreased impulses per MN burst (Table 1) and increased PMN burst frequency (Table 2), that were not significantly changed by the two noninvasive protocols. Although these specific effects could reflect effects of axonal injury or damage to regulatory fibers, we propose that the majority of effects observed with trunk ligature are attributable to the functional separation of the MNs and PMNs, as postulated by previous investigators (Tazaki and Cooke 1983a–c).

Intrinsic burst activity of MNs. Our results indicate that the CG MNs exhibit spontaneous repetitive burst activity when disengaged from the PMNs (Table 1). Intrinsic repetitive MN bursting was initially suggested by experiments in which portions of the lobster CG were crushed or sectioned (Connor 1969; Matsui et al. 1977; Maynard 1955; Watanabe 1958). Tazaki and Cooke used trunk ligatures to dissociate MN and PMN activity in the crab (*P. sanguinolentus*; 1983a) and the lobster (*Homarus americanus*; 1983b). As observed here, following ligature near the midpoint of the CG trunk in *Portunus*,

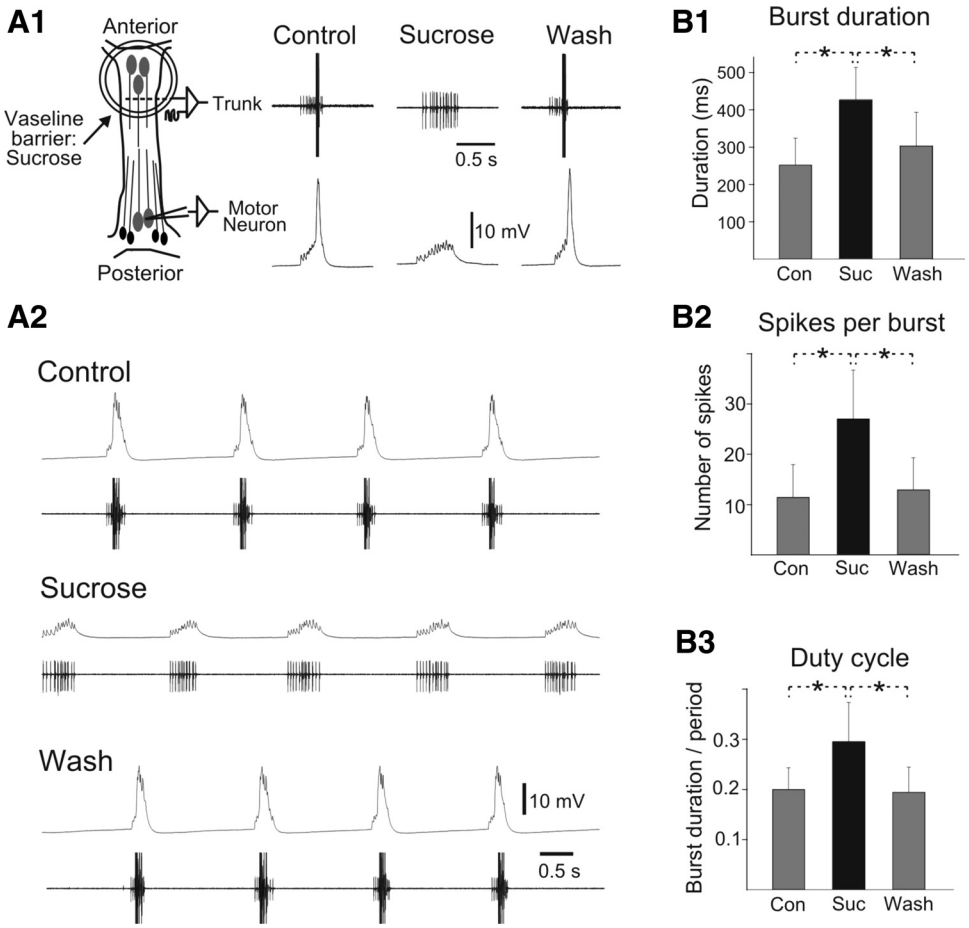

Fig. 7. Effect of silencing MN activity with sucrose (Suc). A_1 sucrose (750 mM) was introduced within a Vaseline barrier surrounding the anterior end of the CG. Ganglion activity was recorded intracellularly from a posterior MN and extracellularly from the ganglion trunk between wire electrodes placed within and outside of the barrier. Large MN impulses observed in the extracellular recording were eliminated in the presence of sucrose. A_2: the posterior MN continued to exhibit rhythmic depolarizing potentials corresponding to PMN bursts recorded from the trunk. Following 10- to 15-min wash with normal saline, the MN impulses were restored. B_1: summary data from 9 experiments show that the duration of PMN bursts was significantly (ANOVA; $F_{2,24} = 10.500$) increased following silencing the MN with sucrose. B_2: group data from 10 experiments show that the number of PMN impulses per burst was significantly (ANOVA; $F_{2,27} = 12.525$) and reversibly increased following silencing the MN with sucrose. B_3: the increased frequency (A_2) and burst duration (B_1) contribute to producing a significant increase in the duty cycle of PMN bursting (ANOVA; $F_{2,27} = 9.261$). $^*P < 0.05$, Holm-Sidak pairwise post hoc tests.

anterior MNs exhibited rhythmic bursts that were not preceded by detectable synaptic activity (Tazaki and Cooke 1983a). In *Homarus*, where MNs are more distributed, spontaneous bursting was demonstrated in a single MN isolated by three ligatures from the remainder of the CG (Tazaki and Cooke 1983b). Tazaki and Cooke (1983b) noted that the spontaneous bursting of MNs following ligature resembled their activity during the onset of TTX poisoning of the CG and proposed that both treatments were disclosing the intrinsic activity of MNs in the absence of PMN input. They recognized, however, the limitations of ligature protocols and cautioned that it was "not possible to rigorously exclude the participation of distal elements of small cells in this activity." Intrinsic MN oscillatory activity was also observed in a cell culture study in which MNs of the shore crab (*Carcinus maenas*) were shown to produce rhythmic bursting 1 day after complete isolation from the ganglion using an enzymatic protocol (Saver et al. 1999). Our findings, which include noninvasive and reversible treatments (local TTX and sucrose application), thus support previous investigations that attributed repetitive bursting to CG MNs when disengaged from PMN influence.

Intrinsic burst activity of PMNs. The intrinsic capacity of PMNs to produce repetitive bursting was initially observed in studies in which ganglia were crushed or transected (Mayeri 1973a). Ligatures of the *Portunus* CG also provided evidence that PMNs continue to burst following disengagement from MN activity (Tazaki and Cooke 1983a). These experiments were facilitated by the favorable functional topography of the crab CG, in which chemical synaptic signaling and active MN responses occur in the anterior portion of the ganglion (Mirolli et al. 1987; Tazaki and Cooke 1979a, 1983a). Ligatures near the middle of the trunk therefore render the posterior MNs silent, allowing them to serve as a monitor of PMN activity via their electrotonic coupling (Miller et al. 1984; Tazaki and Cooke 1983a; Figs. $2A_3$, 5, 7, and 9 of this paper).

Saver et al. (1999) found that PMN cells isolated from the CG of *C. maenas* and cultured overnight exhibited repetitive tonic spiking rather than bursts. This observation led to the proposal that PMN burst activity in the CG was a consequence of network interactions (Saver et al. 1999). Other studies, however, provided evidence supporting the intrinsic capacity of PMNs in other species to produce bursts. Tazaki and Cooke (1983c) demonstrated TTX-resistant DPs in the PMNs of *P. sanguinolentus* and noted that their form could explain differences between the firing patterns of PMNs vs. MNs. Moreover, in *Portunus* and *Podophthalmus vigil* MNs silenced by TTX, Miller et al. (1984) recorded electrically coupled repetitive PMN DPs that were conditional on the presence of dopamine. Berlind (1989) used a two-chamber perfusion system to silence the MNs of the *Homarus* CG with TTX, revealing repetitive PMN bursts that were recorded with extracellular trunk electrodes. In the present study, the properties of spontaneous PMN bursts recorded extracellularly from the CG trunk of *Callinectes* after silencing its MNs with either TTX or sucrose were substantiated by intracellular monitoring of PMN activity via its strong coupling to posterior MNs in the crab

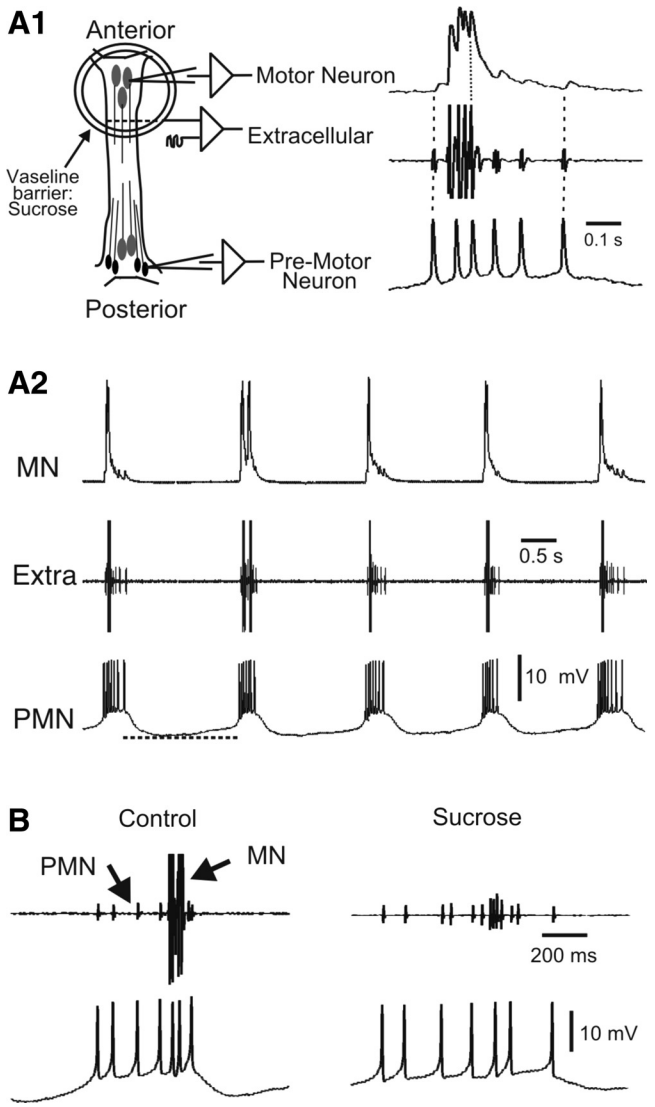

Fig. 8. Effect of silencing MN activity assessed in an individual PMN. A_1: intracellular recording from an anterior MN (*top* record) and posterior PMN (*bottom* record). Each PMN impulse corresponds to a spike recorded extracellularly from the ganglion trunk (*middle* record) and to an EPSP recorded in the MN (dashed lines). A_2: PMN firing precedes and follows MN firing during each burst. The interburst interval of the PMN possesses a prominent depolarizing ramp or pacemaker potential (underscored by dashed line) that is not observed in the MN. *B*: comparison of a PMN burst before and during block of MN firing. Under control conditions, the highest frequency of PMN firing occurred during the MN burst. When MN impulses were blocked by application of sucrose to the anterior region of the CG, the frequency of PMN firing was reduced, and the burst duration was prolonged. Extra, extracellular recording.

CG. Collectively, these findings indicate that the PMNs of most species possess intrinsic burst-forming DPs and that their autonomous activity consists of repetitive bursting.

Feedforward control of motor patterns. The present investigation and the studies reviewed above support a model of the *Callinectes* CG composed of two classes of spontaneously bursting neurons with distinct endogenous rhythms (Fig. 10, *top*). The intrinsic burst frequency of the PMNs (40–60 bpm) disclosed after silencing the MNs with either TTX or sucrose is significantly greater than that of the MNs (10–20 bpm) observed after silencing the PMNs. This finding, coupled with the presence of excitatory PMN-to-MN synaptic signaling in crab CGs (Berlind 1982; Tazaki 1967; Tazaki and Cooke 1979a; this study), is consistent with the long-held designation of the PMNs as functional CG pacemakers under most conditions (Hagiwara and Bullock 1957; Hartline and Cooke 1969; Mayeri 1973a,b; Tazaki and Cooke 1979a; but see Sullivan and Miller 1984). Further support for this role was disclosed in a limited number of intracellular recordings from the PMNs of *Callinectes*. These recordings revealed *1*) interburst ramp or pacemaker potentials that were significantly steeper than those of MNs, *2*) PMN impulses and their associated EPSPs in the MNs that preceded MN firing during each burst, and *3*) no evidence for impulse-mediated MN-to-PMN signaling. All of these findings agree with observations in another portunid crab *P. sanguinolentus* (Tazaki and Cooke 1979a, 1983a,c).

Tazaki and Cooke (1983a) used a pressure-block protocol achieved by partial tightening of a trunk ligature to assess the contribution of impulse-mediated chemical signaling to MN burst formation in *Portunus*. Following such partial ligatures, they observed that the anterior MNs exhibited rhythmic spontaneous bursts that were reduced in duration compared with control conditions. Our experiments in which sucrose was applied to the middle of the *Callinectes* CG trunk support their conclusion that, although chemical EPSPs normally trigger MN bursts (see previous text), they are not required for burst initiation (Tazaki and Cooke 1983a). Unlike the ligature protocols, however, the sucrose technique permitted rapid restoration of impulse conduction along the CG trunk, strengthening the assertion that the MN bursting observed in their absence does not reflect axonal injury or firing of regulatory fibers.

In contrast to the decreased MN burst duration observed after disengagement from PMN signals, the amplitude of the slow potential underlying MN bursts was frequently increased. Such increased MN burst amplitudes were previously observed following partial ligature or during the onset of TTX actions in the CGs of *Portunus* and *Homarus* (Tazaki and Cooke 1983a,c). It was proposed that the synaptic conductance change produced by the neurotransmitter-activated channels could partially shunt the depolarizing currents that give rise to the MN DP, causing a reduction or delay in the activation of the voltage-dependent K^+ current responsible for its termination (Tazaki and Cooke 1983a,c). To summarize, our findings indicate that impulse-mediated feedforward signaling serves *1*) to trigger MN bursts more rapidly than their endogenous frequency, *2*) to prolong the duration of the depolarizing drive for MN bursts beyond the duration of their intrinsic DPs, and *3*) to reduce the amplitude of the MN bursts below the magnitude of their intrinsic DPs (Fig. 10, *bottom*).

Feedback control of motor patterns. The role of electrotonic feedback in the control of CG motor patterns was suggested by early studies in which current injection into individual MNs was shown to alter the activity of the entire network (Matsui et al. 1977; Watanabe 1958; Watanabe and Bullock 1960). Such MN-to-PMN coupling was directly demonstrated with intracellular recording in the crab (*P. sanguinolentus*) CG by Tazaki and Cooke (1979a). In a study of phase-response relations using current pulses injected into *Portunus* MNs, Benson (1980) demonstrated that the CG acted as a single relaxation oscillator that was fully reset following each occurrence of a complete MN burst. It was also shown that application of the neuromodulator octopamine (OA; 10^{-5} M) re-

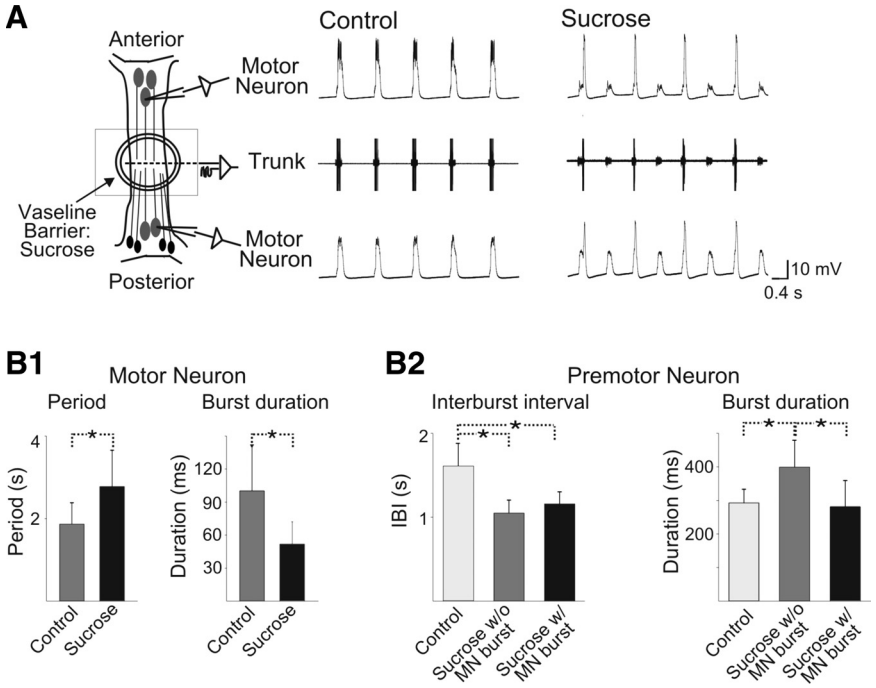

Fig. 9. Elimination of impulse-mediated PMN-to-MN signaling reveals contribution of electrical coupling to generation of motor patterns. *A*: sucrose was placed within a Vaseline pool constructed around the middle ⅓ of the ganglion trunk, whereas spontaneous activity was recorded intracellularly from an anterior MN and a posterior MN. Extracellular recording provided a monitor of ganglion trunk activity. Before sucrose application (control), slow burst-forming potentials and impulses in the anterior MN were larger than those recorded in the posterior MN, supporting their origin in the anterior CG. After replacement of the solution within the partition with sucrose, the PMNs continued to burst (sucrose, trunk recording). The depolarizing potentials produced by PMN bursts were larger in the posterior MNs compared with the anterior MNs, supporting the predominance of PMN-to-MN electrical coupling in the posterior CG (see also Tazaki and Cooke 1983a). Alternate PMN bursts elicited brief MN bursts, which again were larger in the anterior MN. B_1: group data summarizing the effects of midtrunk sucrose treatment on MN burst activity. Elimination of impulse conduction through the CG trunk resulted in an increase in the period of MN bursting ($t = 2.266$, $P < 0.05$) and a decrease in the MN burst duration ($t = 2.795$, $P < 0.05$). *$P < 0.05$, Student's *t*-test, 2-tailed. B_2: group data summarizing the effects of midtrunk sucrose treatment on PMN burst activity. Elimination of impulse conduction through the CG trunk resulted in a decrease in the interburst interval (IBI) of PMN bursting whether or not MN bursts were elicited ($F_{2,14} = 12.465$, $P < 0.05$). The duration of PMN bursting was only prolonged when MN bursts were not elicited ($F_{2,14} = 4.743$, $P < 0.05$). *$P < 0.05$, Holm-Sidak pairwise post hoc tests. w/, With; w/o, without.

duced the reliability with which PMN synaptic input was able to elicit full MN bursting (Benson 1980). In those instances when MN bursts were not triggered, the PMN burst duration and subsequent IBI both were reduced. Our results support the hypothesis that electrotonic feedback from MNs reinforces PMN intraburst firing and contribute to the duration of the subsequent IBI. They differ, however, from the findings of Benson (1980) in one respect, i.e., our observation that MN bursts curtail rather than prolong the intrinsic duration of PMN bursts (Fig. 10). This may represent species differences (*Callinectes* vs. *Portunus*) or may reflect distinct experimental protocols. In the present study, TTX and sucrose were applied selectively to the MNs, whereas in the earlier investigation OA was applied to the entire CG and may have included direct actions on the PMNs.

The inverse relation between burst rate and burst duration that is commonly observed in the CG has been attributed to the MN-to-PMN feedback described above (see Cooke 2002). Benson (1980) accounted for the correlation observed between MN burst duration and the subsequent IBI observed in his reset experiments in terms of the ionic model of the DP advanced by Tazaki and Cooke (1979b,c; 1990). Specifically, Ca^{2+} that enters the MN during a burst activates a Ca^{2+}-dependent K^+ current that contributes to the subsequent PMN IBI via electrotonic feedback. Strong experimental support for the predominance of nonspiking signals in the MN-to-PMN feedback was

Table 1. *Comparison of 3 protocols used to examine intrinsic properties of CG motor neurons*

	Experimental Protocol					
	Ligature		TTX		Sucrose	
MN Burst Parameter	Control	Exp.	Control	Exp.	Control	Exp.
Burst duration, ms	135 ± 46	30 ± 12*	166 ± 83	45 ± 21*	94 ± 26	48 ± 26*
Frequency, bpm	35.2 ± 5.4	21.9 ± 5.8*	32.7 ± 7.9	18.8 ± 6.3*	35.9 ± 7.8	13.6 ± 6.0*
Duty cycle	0.07 ± 0.03	0.03 ± 0.01*	0.08 ± 0.04	0.02 ± 0.01*	0.06 ± 0.04	0.01 ± 0.00*
Spikes per burst	5.3 ± 2.1	3.1 ± 1.5*	7.3 ± 2.4	7.2 ± 3.4	6.4 ± 0.9	6.3 ± 2.4

Values are means ± SE. *$P < 0.05$, Student's *t*-test or Holm-Sidak pairwise post hoc tests. CG, cardiac ganglion; MN, motor neuron; Extra., extracellular recording; bpm, bursts per minute.

Table 2. *Comparison of 3 protocols used to examine intrinsic properties of CG premotor neurons*

	Experimental Protocol					
	Ligature		TTX		Sucrose	
PMN Burst Parameter	Control	Exp.	Control	Exp.	Control	Exp.
Burst duration, ms	310 ± 85	604 ± 245*	273 ± 86	445 ± 130*	245 ± 70	415 ± 84*
Frequency, bpm	31.5 ± 3.5	61.3 ± 18.3*	33.1 ± 10.2	42.0 ± 11.1	32.0 ± 10.8	40.0 ± 14.3
Duty cycle	0.16 ± 0.05	0.55 ± 0.12*	0.20 ± 0.05	0.37 ± 0.10*	0.20 ± 0.04	0.30 ± 0.08*
Spikes per burst	7.3 ± 1.5	14.5 ± 2.6*	13.3 ± 6.9	26.5 ± 7.1*	11.5 ± 6.4	27.0 ± 9.7*

Values are means ± SE. *$P < 0.05$, Student's *t*-test or Holm-Sidak pairwise post hoc tests. PMN, premotor neuron.

provided by Berlind (1989) who used local application of TTX and proctolin in the lobster CG to elicit MN DPs while recording PMN impulses from the CG trunk. These experiments demonstrated that all effects of feedback, i.e., augmented PMN intraburst firing, prolonged PMN bursts, and prolongation of the subsequent IBI, occurred in the absence of MN impulses and could be attributed to the electrotonic flow of the currents associated with the DPs and their afterpotentials (Berlind 1989). Our findings, including our inability to detect rapid MN-to-PMN signals in the few intracellular recordings achieved, support the attribution of MN-to-PMN feedback to low-pass electrotonic coupling of the currents that produce the MN DP and its associated afterpotentials. Again, however, our experiments indicate that this feedback serves to curtail rather than prolong PMN bursting as observed by Berlind (1989) in the lobster (Fig. 10). As electrical coupling is known to be stronger in the crab CG, we attribute this difference to a greater feedback influence by the voltage-dependent K^+ current that terminates MN DPs (Tazaki and Cooke 1979c, 1983b, 1986, 1990).

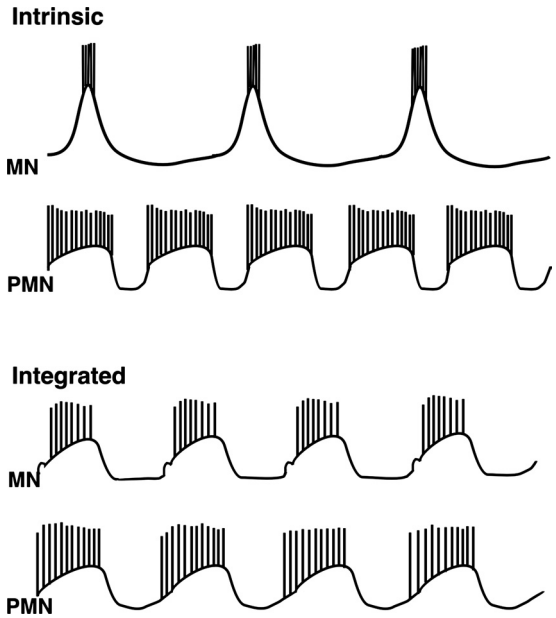

Fig. 10. Schematic summary of the findings of this study. *Top* records: following disengagement with 3 experimental protocols (ligature, TTX, and sucrose), CG MNs and PMNs both exhibit spontaneous intrinsic burst activity. *Bottom*: in the integrated CG, parameters of the MN bursts (frequency, duration, and impulses per burst) are all increased compared with their intrinsic pattern. Parameters of the PMN bursts (frequency, duration, and impulses per burst) are all decreased compared with their intrinsic pattern. The presence of feedforward and feedback signaling thus causes all parameters of the motor patterns produced by the CG to take on intermediate values that lie between the intrinsic burst parameters of its constituent neurons.

Redundancy, coupling, and feedback: consequences and generality. Our experiments indicate that all neurons in the *Callinectes* CG possess endogenous rhythm-generating and burst-generating capabilities (see Cooke 2002). Getting (1989) proposed that CPG circuits controlling continuous actions that are vital to survival are more likely to contain endogenously bursting neurons than circuits that control more episodic movement patterns. This hypothesis gains support from studies showing that crustacean stomatogastric rhythms, the leech heartbeat, and vertebrate respiratory rhythms are driven by core oscillatory bursting neurons (Cymbalyuk et al. 2002; Miller and Selverston 1982; Rekling and Feldman 1998; Selverston et al. 2009). Many repetitive actions that occur more intermittently, such as leech and lamprey swimming, gastropod feeding, and mammalian locomotion, are controlled by CPGs in which rhythmicity reflects network interactions rather than endogenously oscillating neurons (Elliott and Susswein 2002; Friesen and Kristan 2007; Grillner et al. 2008; Kiehn 2006). The redundancy of endogenous oscillator neurons in the CG may contribute to its extraordinary reliability and fault tolerance (Cooke 2002; Maynard 1960; Sivan et al. 1999). Although this organization suggests that repetitive burst activity reflects the default status of the *Callinectes* CG, such conclusions must remain tentative in view of its natural conditions within the heart where it is influenced by feedback from myocardial contractions (García-Crescioni et al. 2010; Sakurai and Wilkens 2003), regulatory fibers originating from the CNS (Fort et al. 2004, 2007a), and numerous blood-borne neuromodulators (Cooke and Sullivan 1982; McGaw et al. 1995; Fort et al. 2004, 2007a,b).

Compartmentalization of signaling contributes to the function of several model CPGs (Dickinson et al. 1981; Evans et al. 2008; Hurwitz et al. 1994; Nusbaum 1994). For both groups of neurons in the CG, distal signals are transmitted by impulse-mediated chemical synapses. In the case of the MNs, these signals occur as discrete excitatory junction potentials at the myocardium (Anderson and Cooke 1971; Florey and Rathmayer 1990), whereas the PMN EPSPs are transmitted to the MNs in the synaptic integrative zone in the anterior region of the CG. In contrast, local signals are dominated by the electrotonic flow of currents associated with the nonpropagating burst-forming DP. These include the feedforward PMN signals to the posterior MNs and the MN-to-PMN electrotonic feedback. Local intraganglionic signals are similarly transmitted by slow burst-forming potentials in the stomatogastric ganglion where they consist of both electrotonic and inhibitory chemical

components (Graubard et al. 1980; Hartline and Graubard 1992; Marder and Eisen 1983a,b).

Finally, the compartmentalization of signaling enables the CG MNs to transmit simultaneous feedforward and feedback information. The feedback to PMNs provides a copy of the efferent signals that are being transmitted to generate each contraction. Although this electrotonic feedback possesses an analog form, it can faithfully approximate motor pattern parameters (burst frequency, burst duration, and impulses per burst) because it originates from the same MN currents that contribute to shaping that motor activity. As a result of this circuit architecture, all parameters of the motor patterns that emerge from the CG are influenced by the intrinsic properties of both of its constituent neuron groups. Notably, however, none of these parameters are dictated by the endogenous properties of either group. The presence of such syncytial or reticular qualities within the microcircuits that comprise more complex nervous systems could enhance their fidelity, reliability, and information-processing capabilities.

GRANTS

This investigation was supported by National Institute of General Medical Sciences Minority Biomedical Research Support Grants SC3 GM-087200 and GM-061838. Additional infrastructure support came from National Center for Research Resources Research Centers in Minority Institutions Grant RR-03051, U.S. Department of Defense Grant 52680-RT-ISP, and National Science Foundation Grant DBI-0115825.

DISCLOSURES

No conflicts of interest, financial or otherwise, are declared by the author(s).

REFERENCES

Abbott NH, Moreton RB, Pichon Y. Electrophysiological analysis of potassium and sodium movements in crustacean nervous system. *J Exp Biol* 63: 85–115, 1975.

Alexandrowicz JS. The innervation of the heart of the *Crustacea*. *I Decapoda Q J Microscop Sci* 75: 181–249, 1932.

Anderson M, Cooke IM. Neural activation of the heart of the lobster, *Homarus americanus*. *J Exp Biol* 55: 449–468, 1971.

Ball JM, Franklin CC, Tobin AE, Schulz DJ, Nair SS. Coregulation of ion channel conductances preserves output in a computational model of a crustacean cardiac motor neuron. *J Neurosci* 30: 8637–8649, 2010.

Bennett MV. Neoreticularism and neuronal polarization. *Prog Brain Res* 136: 189–201, 2002.

Bennett MV, Zukin RS. Electrical coupling and neuronal synchronization in the mammalian brain. *Neuron* 41: 495–511, 2004.

Benson JA. Burst reset and frequency control of the neuronal oscillators in the cardiac ganglion of the crab, *Portunus sanguinolentus*. *J Exp Biol* 87: 285–313, 1980.

Berlind A. Spontaneous and repetitive driver potentials in crab cardiac ganglion neurons. *J Comp Physiol A* 149: 263–276, 1982.

Berlind A. Feedback from motor neurones to pacemaker neurones in lobster cardiac ganglion contributes to regulation of burst frequency. *J Exp Biol* 141: 277–294, 1989.

Bullock TH, Bennett MV, Johnston D, Josephson R, Marder E, Fields RD. The neuron doctrine, redux. *Science* 310: 791–793, 2005.

Cohen AH. The role of heterarchical control in the evolution of the central pattern generator for locomotion. *Brain Behav Evol* 40: 112–124, 1992.

Connor JA. Burst activity and cellular interaction in the pacemaker ganglion of the lobster heart. *J Exp Biol* 50: 275–295, 1969.

Connors BW, Long MA. Electrical synapses in the mammalian brain. *Annu Rev Neurosci* 27: 393–410, 2004.

Cooke IM. Studies on the crustacean cardiac ganglion. *Comp Biochem Physiol C* 91: 205–218, 1988.

Cooke IM. Reliable, responsive pacemaking and pattern generation with minimal cell numbers: the crustacean cardiac ganglion. *Biol Bull* 202: 108–136, 2002.

Cooke IM, Sullivan RE. Hormones and neurosecretion. In: *The Biology of Crustacea*, edited by Bliss D, Atwood H, and Sandman D. New York: Academic Press, 1982, vol. 3, p. 205–290.

Cymbalyuk GS, Gaudry Q, Masino MA, Calabrese RL. Bursting in leech heart interneurons: cell-autonomous and network-based mechanisms. *J Neurosci* 22: 10580–10592, 2002.

Delgado J, Oyola E, Miller MW. Localization of GABA- and glutamate-like immunoreactivity in the cardiac ganglion of the lobster *Panulirus argus*. *J Neurocytol* 29: 605–619, 2001.

Dickinson PS, Nagy F, Moulins M. Interganglionic communication by spiking and nonspiking fibers in the same neuron. *J Neurophysiol* 45: 1125–1138, 1981.

Elliott CJ, Susswein AJ. Comparative neuroethology of feeding control in mollusks. *J Exp Biol* 205: 877–896, 2002.

Evans CG, Kang T, Cropper EC. Selective spike propagation in the central processes of an invertebrate neuron. *J Neurophysiol* 100: 2940–2947, 2008.

Florey E, Rathmayer M. Facilitation and potentiation of transmitter release at neuromuscular synapses in the heart of Squilla mantis: functional and theoretical implications. In: *Frontiers in Crustacean Neurobiology, Advances in Life Sciences*, edited by Wiese K, Krenz W-D, Tautz H, and Mulloney B. Basel: Birkhäuser Verlag, 1990, p. 330–337.

Fort TJ, Brezina V, Miller MW. Modulation of an integrated central pattern generator-effector system: dopaminergic regulation of cardiac activity in the blue crab *Callinectes sapidus*. *J Neurophysiol* 92: 3455–3470, 2004.

Fort TJ, Brezina V, Miller MW. Regulation of the crab heartbeat by FMRFamide-like peptides: multiple interacting effects on center and periphery. *J Neurophysiol* 98: 2887–2902, 2007a.

Fort TJ, García Crescioni K, Agricola HJ, Brezina V, Miller MW. Regulation of the crab heartbeat by crustacean cardioactive peptide (CCAP): central and peripheral actions. *J Neurophysiol* 97: 3407–3420, 2007b.

Friesen WO, Kristan WB. Leech locomotion: swimming, crawling, and decisions. *Curr Opin Neurobiol* 17: 704–711, 2007.

Friesen WO, Stent GS. Neural circuits for generating rhythmic movements. *Annu Rev Biophys Bioeng* 7: 37–61, 1978.

García-Crescioni K, Fort TJ, Stern E, Brezina V, Miller MW. Feedback from peripheral musculature to central pattern generator in the neurogenic heart of the crab *Callinectes sapidus*: role of mechanosensitive dendrites. *J Neurophysiol* 103: 83–96, 2010.

Getting PA. Emerging principles governing the operation of neural networks. *Annu Rev Neurosci* 12: 185–204, 1989.

Getting PA, Willows AO. Modification of neuron properties by electrotonic synapses. II. Burst formation by electrotonic synapses. *J Neurophysiol* 37: 858–868, 1974.

Graubard K, Raper JA, Hartline DK. Graded synaptic transmission between spiking neurons. *Proc Natl Acad Sci USA* 77: 3733–3735, 1980.

Grillner S, Graybiel AM. *Microcircuits: The Interface Between Neurons and Global Brain Function*. Cambridge, MA: MIT Press, 2006.

Grillner S, Wallén P, Saitoh K, Kozlov A, Robertson B. Neural bases of goal-directed locomotion in vertebrates–an overview. *Brain Res Rev* 57: 2–12, 2008.

Guillery RW. Relating the neuron doctrine to the cell theory. Should contemporary knowledge change our view of the neuron doctrine? *Brain Res Rev* 55: 411–421, 2007.

Hagiwara S. Nervous activities of the heart in *Crustacea*. *Ergeb Biol* 24: 287–311, 1961.

Hagiwara S, Bullock TH. Intracellular potentials in pacemaker and integrative neurons of the lobster cardiac ganglion. *J Cell Comp Physiol* 50: 25–47, 1957.

Harris-Warrick RM, Marder E. Modulation of neural networks for behavior. *Annu Rev Neurosci* 14: 39–57, 1991.

Hartline DK, Cooke IM. Postsynaptic membrane response predicted from presynaptic input pattern in lobster cardiac ganglion. *Science* 164: 1081–1082, 1969.

Hartline DK, Graubard K. Cellular and synaptic properties in the crustacean stomatogastric nervous system. In: *Dynamic Biological Networks: The Stomatogastric Nervous System*, edited by Harris-Warrick R, Marder E, Selverston AI, and Moulins M. Cambridge, MA: MIT Press, 1992, p. 31–85.

Hokkanen JE. Chaotic or periodic variation? Looking at *Crustacea* hearts. *J Theor Biol* 203: 451–454, 2000.

Hooper SL, DiCaprio RA. Crustacean motor patern generator networks. *Neurosignals* 13: 50–69, 2004.

Hurwitz I, Goldstein RS, Susswein AJ. Compartmentalization of pattern-initiating and motor function in the B31 and B32 neurons of the buccal ganglia of *Aplysia californica*. *J Neurophysiol* 71: 1514–1527, 1994.

Johnston D, Christie BR, Frick A, Gray R, Hoffman DA, Schexnayder LK, Watanabe S, Yuan LL. Active dendrites, potassium channels and synaptic plasticity. *Philos Trans R Soc Lond B Biol Sci* 358: 667–674, 2003.

Kiehn O. Locomotor circuits in the mammalian spinal cord. *Annu Rev Neurosci* 29: 279–306, 2006.

Krajniak KG. The identification and structure-activity relations of a cardioactive FMRFamide-related peptide from the blue crab *Callinectes sapidus*. *Peptides* 12: 1295–1302, 1991.

Kruger L, Otis TS. Whither withered Golgi? A retrospective evaluation of reticularist and synaptic constructs. *Brain Res Bull* 72: 201–207, 2007.

Manor Y, Rinzel J, Segev I, Yarom Y. Low-amplitude oscillations in the inferior olive: a model based on electrical coupling of neurons with heterogeneous channel densities. *J Neurophysiol* 77: 2736–2752, 1997.

Marder E. Electrical synapses: beyond speed and synchrony to computation. *Curr Biol* 8: R795–R797, 1998.

Marder E, Calabrese RL. Principles of rhythmic motor pattern generation. *Physiol Rev* 76: 687–717, 1996.

Marder E, Eisen JS. Transmitter identification of pyloric neurons: electrically coupled neurons used different transmitters. *J Neurophysiol* 51: 1345–1361, 1984a.

Marder E, Eisen JS. Electrically coupled pacemaker neurons respond differently to same physiological inputs and neurotransmitters. *J Neurophysiol* 51: 1362–1374, 1984b.

Matsui K, Kuwusawa K, Kuramoto T. Periodic bursts in large cell preparations of the lobster cardiac ganglion (*Panulirus japonicus*). *Comp Biochem Physiol* 56A: 313–324, 1977.

Mayeri E. Functional organization of the cardiac ganglion of the lobster, *Homarus americanus*. *J Gen Physiol* 62: 448–472, 1973a.

Mayeri E. A relaxation oscillator description of the burst generating mechanism in the cardiac ganglion of the lobster, *Homarus americanus*. *J Gen Physiol* 62: 473–478, 1973b.

Maynard DM. Activity in a crustacean ganglion. II. Pattern and interaction in burst formation. *Biol Bull* 109: 420–436, 1955.

Maynard DM. Circulation and heart function. In: *The Physiology of Crustaceans*, edited by Waterman TH. New York: Academic Press, 1960, vol. 1, p. 161–226.

McGaw IJ, Wilkens JL, McMahon BR, Airriess CN. Crustacean cardioexcitatory peptides may inhibit the heart in vivo. *J Exp Biol* 198: 2547–2550, 1995.

Miller JP, Selverston AI. Mechanisms underlying pattern generation in lobster stomatogastric ganglion as determined by selective inactivation of identified neurons. II. Oscillatory properties of pyloric neurons. *J Neurophysiol* 48: 1378–1391, 1982.

Miller MW, Benson JA, Berlind A. Excitatory effects of dopamine on the cardiac ganglia of the crabs *Portunus sanguinolentus* and *Podophthalmus vigil*. *J Exp Biol* 108: 97–118, 1984.

Miller MW, Sullivan RE. Some effects of proctolin on the cardiac ganglion of the Maine lobster, *Homarus americanus* (Milne Edwards). *J Neurobiol* 12: 629–639, 1981.

Mirolli M, Cooke IM, Talbott SR, Miller MW. Structure and localization of synaptic complexes in the cardiac ganglion of a portunid crab. *J Neurocytol* 16: 115–130, 1987.

Nusbaum MP. Presynaptic control of neurones in pattern-generating networks. *Curr Opin Neurobiol* 4: 909–914, 1994.

Pearson KG. Common principles of motor control in vertebrates and invertebrates. *Annu Rev Neurosci* 16: 265–297, 1993.

Pearson KG. Neural adaptation in the generation of rhythmic behavior. *Annu Rev Physiol* 62: 723–753, 2000.

Perrins R, Weiss KR. Compartmentalization of information processing in an *Aplysia* feeding circuit interneuron through membrane properties and synaptic interactions. *J Neurosci* 18: 3977–3989, 1998.

Rabbah P, Golowasch J, Nadim F. Effect of electrical coupling on ionic current and synaptic potential measurements. *J Neurophysiol* 84: 519–530, 2005.

Rekling JC, Feldman JL. PreBötzinger complex and pacemaker neurons: hypothesized site and kernel for respiratory rhythm generation. *Annu Rev Physiol* 60: 385–405, 1998.

Russell DF. CNS control of pattern generators in the lobster stomatogastric nervous system. *Brain Res* 177: 598–602, 1979.

Sakurai A, Wilkens JL. Tension sensitivity of the heart pacemaker neurons in the isopod crustacean *Ligia pallasii*. *J Exp Biol* 206: 105–115, 2003.

Saver MA, Wilkens JL, Syed NI. In situ and in vitro identification and characterization of cardiac ganglion neurons in the crab, *Carcinus maenas*. *J Neurophysiol* 81: 2964–2976, 1999.

Selverston AI, Szücs A, Huerta R, Pinto R, Reyes M. Neural mechanisms underlying the generation of the lobster gastric mill motor pattern. *Front Neural Circuits* 3: 12, 2009.

Selverston AI. Invertebrate central pattern generator circuits. *Philos Trans R Soc Lond B Biol Sci* 365: 2239–2245, 2010.

Selverston AI, Ayers J. Oscillations and oscillatory behavior in small neural circuits. *Biol Cybern* 95: 537–554, 2006.

Shepherd GM and Grillner S. (editors). *Handbook of Brain Microcircuits*. New York: Oxford Univ., 2010.

Shimahara T. The inhibitory post-synaptic potential in the cardiac ganglion cell of the lobster, *Panulirus japonicus*. *Sci Rep Tokyo Kyoiku Daigaku B* 14: 9–26, 1969.

Sivan E, Parnas H, Dolev D. Fault tolerance in the cardiac ganglion of the lobster. *Biol Cybern* 81: 11–23, 1999.

Soto-Treviño C, Rabbah P, Marder E, Nadim F. Computational model of electrically coupled, intrinsically distinct pacemaker neurons. *J Neurophysiol* 94: 590–604, 2005.

Stern E, Fort TJ, Miller MW, Peskin CS, Brezina V. Decoding modulation of the neuromuscular transform. *Neurocomputing* 70: 1753–1758, 2007.

Stern E, García-Crescioni K, Miller MW, Peskin CS, Brezina V. A method for decoding the neurophysiological spike-response transform. *J Neurosci Methods* 184: 337–356, 2009.

Sullivan RE, Miller MW. Dual effects of proctolin on the rhythmic burst activity of the cardiac ganglion. *J Neurobiol* 15: 173–196, 1984.

Szücs A, Huerta R, Rabinovich MI, Selverston AI. Robust microcircuit synchronization by inhibitory connections. *Neuron* 61: 439–453, 2009.

Tameyasu T. Intracellular potentials in the small cells and cellular interaction in the cardiac ganglion of the lobster, *Panulirus japonicus*. *Comp Biochem Physiol* 54A: 191–196, 1976.

Tazaki K. Intracellular potential changes in the cardiac ganglion cell of the crab, *Eriocheir japonicus*. *Sci Rep Tokyo Daigaku* B12: 191–210, 1967.

Tazaki K. The effects of tetrodotoxin on the slow potential and spikes in the cardiac ganglion of a crab, *Eriocheir japonicus*. *Jpn J Physiol* 21: 529–536, 1971.

Tazaki K. The burst activity of different cell regions and intercellular coordination in the cardiac ganglion of the crab, *Eriocheir japonicus*. *J Exp Biol* 57: 713–726, 1972.

Tazaki K, Cooke IM. Currents under voltage clamp of burst-forming neurons of the cardiac ganglion of the lobster. *(Homarusamericanus). J Neurophysiol* 56: 1739–1762, 1986.

Tazaki K, Cooke IM. Spontaneous electrical activity and interaction of large and small cells in the cardiac ganglion of the crab, *Portunus sanguinolentus*. *J Neurophysiol* 42: 975–999, 1979a.

Tazaki K, Cooke IM. Isolation and characterization of slow, depolarizing responses of cardiac ganglion neurons in the crab, *Portunus sanguinolentus*. *J Neurophysiol* 42: 1000–1021, 1979b.

Tazaki K, Cooke IM. The ionic bases of slow depolarizing responses of cardiac ganglion neurons of the crab, *Portunus sanguinolentus*. *J Neurophysiol* 42: 1022–1047, 1979c.

Tazaki K, Cooke IM. Topographical localization of function in the cardiac ganglion of the crab, *Portunus sanguinolentus*. *J Comp Physiol A* 151: 311–328, 1983a.

Tazaki K, Cooke IM. Neural mechanisms underlying rhythmic bursts in crustacean cardiac ganglia. In: *Neural Origin of Rhythmic Movements*, edited by Roberts A and Roberts B. Cambridge, UK: Cambridge Univ. Press, 1983b, vol. 37, p. 129–157.

Tazaki K, Cooke IM. Separation of neuronal sites of driver potential and impulse generation by ligaturing in the cardiac ganglion of the lobster, *Homarus americanus*. *J Comp Physiol A* 151: 329–346, 1983c.

Tazaki K, Cooke IM. Characterization of Ca current underlying burst formation in lobster cardiac ganglion neurons. *J Neurophysiol* 63: 370–384, 1990.

Tobin AE, Cruz-Bermúdez ND, Marder E, Schulz DJ. Correlations in ion channel mRNA in rhythmically active neurons. *PLoS One* 4: e6742, 2009.

Watanabe A. The interaction of electrical activity among neurons of lobster cardiac ganglion. *Jpn J Physiol* 8: 305–318, 1958.

Watanabe A, Bullock TH. Modulation of activity of one neuron by subthreshold slow potentials in another in lobster cardiac ganglion. *J Gen Physiol* 43: 1031–1045, 1960.

Wilson JM, Cowan AI, Brownstone RM. Heterogeneous electrotonic coupling and synchronization of rhythmic bursting activity in mouse Hb9 interneurons. *J Neurophysiol* 98: 2370–2381, 2007.